

# **Individual differences in structural and functional connectivity predict speed of emotion discrimination**

Lars Marstaller<sup>1,2</sup>, Hana Burianová<sup>1,3</sup>, and David C. Reutens<sup>1</sup>

<sup>1</sup>Centre for Advanced Imaging, University of Queensland, Brisbane, Australia

<sup>2</sup>ARC Science of Learning Research Centre, University of Queensland, Brisbane, Australia

<sup>3</sup>Department of Psychology, Swansea University, Swansea, United Kingdom

## **Correspondence should be addressed to:**

Lars Marstaller, PhD

Centre for Advance Imaging

University of Queensland

QLD 4072, AUSTRALIA

[l.marstaller@uq.edu.au](mailto:l.marstaller@uq.edu.au)

Pages: 25

Figures: 5

## Highlights

- Discrimination speed of angry and fearful faces related to separate networks.
- Angry faces are discriminated faster by extended emotional face processing network.
- Fearful faces are discriminated faster by cortical visual-attentional regions.
- Discrimination speed of angry but not fearful faces associated with right amygdala.
- Integrity of inferior longitudinal fasciculus improves threat discrimination speed.

**Abstract**

1  
2 In social interactions, individuals who are slower at differentiating between facial  
3  
4 expressions signalling direct and indirect threat might be at a serious disadvantage.  
5  
6 However, the neurobiological underpinnings of individual differences in face  
7  
8 processing are not yet fully understood. The aim of this study was to use multimodal  
9  
10 neuroimaging to investigate how the speed of emotion recognition is related to the  
11  
12 structural and functional connectivity underlying the differentiation of direct and  
13  
14 indirect threat displays. Our results demonstrate that individuals, who are faster at  
15  
16 discriminating angry faces, engaged areas of the extended emotional system more  
17  
18 strongly than individuals with slower reaction times, showed higher white matter  
19  
20 integrity in the inferior longitudinal fasciculus, as well as stronger functional  
21  
22 connectivity with the right amygdala. In contrast, individuals, who were faster at  
23  
24 discriminating fearful faces, engaged visual-attentional regions outside of the face  
25  
26 processing network more strongly than individuals with slower reaction times,  
27  
28 showed higher white matter integrity in the inferior longitudinal fasciculus, as well as  
29  
30 reduced functional connectivity with the right amygdala. Our findings suggest that the  
31  
32 high survival value of rapid and appropriate responses to threat has defined but  
33  
34 separate neurobiological correlates for angry and fearful facial expressions.  
35  
36  
37  
38  
39  
40  
41  
42  
43  
44  
45

46 **Keywords:** emotion discrimination; structural-functional connectivity; individual  
47  
48 differences  
49  
50  
51  
52  
53  
54  
55  
56  
57  
58  
59  
60  
61  
62  
63  
64  
65

## 1. Introduction

1  
2  
3  
4  
5  
6  
7  
8  
9  
10  
11  
12  
13  
14  
15  
16  
17  
18  
19  
20  
21  
22  
23  
24  
25  
26  
27  
28  
29  
30  
31  
32  
33  
34  
35  
36  
37  
38  
39  
40  
41  
42  
43  
44  
45  
46  
47  
48  
49  
50  
51  
52  
53  
54  
55  
56  
57  
58  
59  
60  
61  
62  
63  
64  
65

Rapid and accurate discrimination of facial expressions of emotion is important for preparing adequate and timely responses in social interactions (Cizek & Kalaska, 2010). Rapid discrimination is particularly important for facial expressions displaying anger and fear, as these emotions signal direct and indirect threat respectively, which might require an immediate fight-or-flight response (Bannerman et al., 2009; Hansen & Hansen, 1988; Lo & Cheng, 2015; Whalen et al., 2001). Previous research has shown that the ability to rapidly discriminate between emotional facial expressions signalling threat depends on the core face-processing network, including inferior occipital gyrus, superior temporal sulcus, and fusiform gyrus, as well as the extended emotional system centered on the amygdala (Haxby et al. 2002; Rossion et al., 2003; Gobbini & Haxby, 2007). During the conscious recognition of threatening emotional facial expressions, the core network and the extended emotional system interact through bidirectional functional connections between the amygdala and the fusiform gyrus (Herrington et al., 2011; Wang et al., 2016). Functional connectivity between fusiform gyrus and amygdala, together with the ability to discriminate emotions depend on white matter pathways within the inferior longitudinal fasciculus (Kleinhans et al., 2008; Koldewyn et al., 2014). This structural-functional relationship allows the amygdala to exert top-down control on the ventral visual pathway during the perception of threat-signalling facial expressions (Amaral, Behniea & Kelly, 2003; Villeumier et al., 2003; De Gelder et al., 2014). Thus, this evidence suggests that rapid discrimination of threat-related emotional facial expressions crucially depends on the functional and structural connectivity between the amygdala and fusiform gyrus and that individuals with less efficient structural and functional connectivity may be at a disadvantage in threat-

1 related social interactions. However, to date, no study has investigated whether the  
2 functional and structural connectivity between the amygdala and fusiform gyrus  
3 affects the speed of emotion discrimination in healthy adults.  
4  
5

6  
7 The objective of this study was to investigate whether individual differences in  
8 structural integrity and functional connectivity between the core and extended  
9 emotional face-processing networks would predict the speed of conscious emotion  
10 discrimination for angry and fearful facial expressions. In particular, we were  
11 interested in the three-way **relation** between structural connectivity, functional  
12 connectivity, and behaviour during an emotion discrimination task that required  
13 participants to match facial expressions of fear or anger. As an indicator of structural  
14 connectivity, we assessed the white matter integrity of the inferior longitudinal  
15 fasciculus (ILF), which constitutes the major white matter pathway along the ventral  
16 visual processing stream, mediating the interactions between the amygdala and the  
17 fusiform gyrus during face processing (Catani et al., 2003; Thomas et al., 2009). As  
18 an indicator of functional connectivity, we used a seed-based approach and covaried  
19 functional activity within the amygdala with task-related activity across the whole  
20 brain. As an indicator of behaviour, we measured reaction times of emotion  
21 discrimination. Based on previous studies, which show that angry and fearful faces  
22 are identified equally fast and that processing of both emotions engages the core and  
23 extended face-processing networks (De Sonneville et al., 2002; Whalen et al., 2001),  
24 we hypothesized that, as a group, participants would (i) be equally fast to match angry  
25 and fearful faces and (ii) engage the core and extended face processing networks for  
26 both facial expressions. Based on the assumption that the discrimination of different  
27 emotional expressions requires the interaction between the amygdala and fusiform  
28 gyrus (Herrington et al., 2011; Wang et al., 2016), we further hypothesized that (iii)  
29  
30  
31  
32  
33  
34  
35  
36  
37  
38  
39  
40  
41  
42  
43  
44  
45  
46  
47  
48  
49  
50  
51  
52  
53  
54  
55  
56  
57  
58  
59  
60  
61  
62  
63  
64  
65

1 for both angry and fearful facial expressions, individuals who discriminate emotions  
2 more rapidly would also have better white matter integrity in the ILF and increased  
3 functional connectivity within and between the core and extended face-processing  
4 networks. More specifically, we hypothesized that shorter reaction times should  
5 correlate with higher FA values as well as connectivity values in the face processing  
6 network.  
7  
8  
9  
10  
11  
12  
13  
14  
15  
16

## 17 **2. Methods**

### 18 *2.1 Participants*

19  
20  
21  
22 28 right-handed adults (14 females, mean age = 26.3 years, age range = 21-34  
23 years) with normal or corrected to normal vision gave written consent to take part in  
24 the experiment, which was approved by the Human Ethics Research Committee of the  
25 University of Queensland. All participants were screened for neuropsychological  
26 disorders, brain damage, and substance abuse. Images were acquired with a Siemens  
27 Magnetom Trio 3T (Siemens Healthcare, Erlangen, Germany) and a standard 32-  
28 channel head coil at the Centre for Advanced Imaging, University of Queensland.  
29  
30  
31  
32  
33  
34  
35  
36  
37  
38  
39  
40

### 41 *2.2 Experimental Procedure*

42  
43  
44 Participants took part in an emotion-matching task adapted from the paradigm  
45 described in Hariri et al. (2000). During each trial, three images were presented, one  
46 in the top and two in the bottom half of the screen using Presentation software  
47 (Neurobehavioral Systems, Inc.). One of the bottom two images was identical to the  
48 top image and participants were asked to identify the image in the bottom half of the  
49 screen that matched the top image by pressing the one of two buttons associated with  
50 the left and right image. Images either showed black elliptical shapes angled at 45° or  
51  
52  
53  
54  
55  
56  
57  
58  
59  
60  
61  
62  
63  
64  
65

1  
2  
3  
4  
5  
6  
7  
8  
9  
10  
11  
12  
13  
14  
15  
16  
17  
18  
19  
20  
21  
22  
23  
24  
25  
26  
27  
28  
29  
30  
31  
32  
33  
34  
35  
36  
37  
38  
39  
40  
41  
42  
43  
44  
45  
46  
47  
48  
49  
50  
51  
52  
53  
54  
55  
56  
57  
58  
59  
60  
61  
62  
63  
64  
65

315° (shapes condition) or facial expressions with a target of angry (angry condition) or fearful facial expressions (fearful condition). During presentation of facial expressions, all pictures were of the same model and always included one fearful and one angry facial expression presented in the bottom row, which makes the two facial expression conditions directly comparable. Reaction times were measured and data from individual trials was removed from the behavioural analysis if they constituted outliers, i.e., a reaction time shorter than 350 ms or longer than 1800 ms.

Image stimuli consisted of 24 pictures selected from the Radboud Faces Database (<http://www.socsci.ru.nl:8180/RaFD2/RaFD>). In each picture, a trained model (young adult Caucasian males and females) displayed either a fearful or an angry facial expression with direct gaze (Langner et al., 2010). Control stimuli consisted of black ellipses angled at 45° or 315° generated by Presentation software. Images were presented in 6 blocks (3 blocks of shapes, 3 blocks of faces), each containing 6 trials. The presentation order of blocks was randomized. At the beginning of each block, an instruction was presented for 3s to either “match the faces” or to “match the shapes”. In each trial, the images were presented for 2s followed by a fixation cross for 1s.

Due to a technical error, the behavioural accuracy of the participants’ responses was not recorded. Observations of participants’ responses during the task suggested that behavioural accuracy was at ceiling and that accuracy would not be an important factor in assessing the **relation** between behaviour, structure, and function. To confirm this observation, we subsequently tested the same paradigm behaviourally in a separate sample of 28 young, right-handed adults (mean age = 22 years, age range = 18-30 years, 19 females). As predicted, participants’ accuracies showed a ceiling effect for each of the three stimulus types: angry faces group mean score = 0.96, SD =

1  
2  
3  
4  
5  
6  
7  
8  
9  
10  
11  
12  
13  
14  
15  
16  
17  
18  
19  
20  
21  
22  
23  
24  
25  
26  
27  
28  
29  
30  
31  
32  
33  
34  
35  
36  
37  
38  
39  
40  
41  
42  
43  
44  
45  
46  
47  
48  
49  
50  
51  
52  
53  
54  
55  
56  
57  
58  
59  
60  
61  
62  
63  
64  
65

0.04; fearful faces group mean score = 1.0, SD = 0.0; and shapes group mean score = 0.94, SD = 0.09. To ensure comparability between the two groups, we further compared their reaction times. A 2 x 3 mixed-design ANOVA of the dependent variable reaction time with a fixed effects factor group (first, second) and a random effects factor stimulus (angry, fearful, shapes) yielded a significant factor of group ( $F(1) = 40.167$ ,  $p < 0.001$ ) and a significant factor of stimulus ( $F(2) = 20.603$ ,  $p < 0.001$ ), but no interaction between factors. Using only data from the second group, two-sided t-tests of the reaction times to different stimulus types showed significantly faster responses to shapes than to angry and fearful facial expressions (both  $t(27) > 6.4$ , both  $p < 0.001$ ) but not between facial expressions ( $t(27) = 0.5$ ,  $p = 0.7$ ). These results replicate the results reported below for the first group although participants in the second group were overall faster across all stimulus types (significant main effect of the factor group). This group difference can be attributed to the different testing conditions because the first group was tested in the MRI whereas the second group was tested in a behavioural laboratory. Taken together, these results confirm that reaction time but not accuracy should be considered an important factor when investigating the **relation** between behaviour, structure, and function during the emotion-matching task.

### 2.3 Image Acquisition

For each participant, a T1-weighted volumetric anatomical MRI was acquired with the following parameters: 176 slices sagittal acquisition MP2RAGE;  $1\text{mm}^3$  isotropic volume; repetition time (TR) = 4000 msec; echo time (TE) = 2.89 msec; flip angle =  $6^\circ$ ; FOV = 256 mm, GRAPPA acceleration factor = 3. Functional images were acquired using a T2\*-weighted echo-planar image pulse sequence with the



1 following parameters: 45 slices; voxel size = 2.5 x 2.5 x 2.7 mm; TR = 3000 msec;  
2 TE = 30 msec; FOV = 192 mm; flip angle = 90°. Diffusion-weighted images with a  
3 high angular resolution (HARDI) were acquired for each participant using a fast echo-  
4 planar sequence with the following parameters: b1-value = 3000 s/mm<sup>2</sup>; 64 gradient  
5 directions; TR = 8600 msec; TE = 109 msec; FOV = 240 mm; 60 slices; voxel size =  
6 2.3 mm isotropic; GRAPPA acceleration factor = 2.  
7  
8  
9  
10  
11  
12  
13  
14  
15  
16

#### 17 *2.4 fMRI Preprocessing & Whole-Brain Analysis*

18  
19 Brain activation was assessed using the blood oxygenation level dependent  
20 (BOLD) effect (Ogawa et al., 1990) with optimal contrast. For functional analysis,  
21 T2\*-weighted images were preprocessed with Statistical Parametric Mapping  
22 software (SPM8; <http://www.fil.ion.ucl.ac.uk/spm>). Images were realigned to a mean  
23 image to correct for head motion and then spatially normalized into standard  
24 stereotaxic space with voxel size of 2 mm<sup>3</sup>, using the Montreal Neurological Institute  
25 (MNI) template. Head movement and rotation did not exceed 1 mm or 1.5° and no  
26 dataset had to be excluded from the analysis. Finally, the functional images were  
27 spatially smoothed with a 6-mm full width half maximum Gaussian kernel.  
28  
29  
30  
31  
32  
33  
34  
35  
36  
37  
38  
39  
40

41 Following preprocessing, images were submitted to whole-brain analysis  
42 using PLS software (PLS, <http://www.rotman-baycrest.on.ca/index.php?section=84>).  
43 PLS analysis proceeds in several steps (McIntosh et al., 1996, 2004; Krishnan et al.,  
44 2011). First, data from individual trials and participants are sorted by condition and  
45 collated into a single data matrix and a second matrix containing task design (for task-  
46 PLS) as well as covariates of interest (seed-PLS) is created. Second, the data and  
47 covariate matrices are mean-centered and normalized. Third, a covariance matrix is  
48 created from the dot product of the data and covariates matrices. Fourth, PLS uses  
49  
50  
51  
52  
53  
54  
55  
56  
57  
58  
59  
60  
61  
62  
63  
64  
65

1 singular value decomposition - a form of principal components analysis – to identify  
2 brain activity patterns related to task conditions (task PLS) and task conditions as well  
3 as seed values (seed PLS). Since PLS analyzes the data in a single analytical step, no  
4 corrections for multiple comparisons are necessary. Singular value decomposition  
5 yields latent variables that relate to the largest dimensions of variation within the data.  
6 Each latent variable consist of a pattern of brain activity, a singular value, and a  
7 matrix of loadings that indicate how each pattern relates to the task design and the  
8 seed values. Fifth, PLS assesses the reliability of the brain activity patterns at each  
9 voxel using a bootstrap estimation of the standard error with 100 iterations. All brain  
10 activity patterns were thresholded at a bootstrap ratio of 2 as this equates to a p-value  
11 of < 0.05. Sixth, PLS calculates a brain score for each experimental condition and  
12 each participant, which indicates how strong a pattern is represented in the  
13 experimental sample (McIntosh et al., 2004). Brain scores therefore represent  
14 individual differences.

### 2.5 White Matter Analysis

36 Structural connectivity was assessed using MRtrix3 software  
37 (<https://github.com/MRtrix3/>) and tools from the FMRIB Software Library (FSL  
38 5.0.6; <http://fsl.fmrib.ox.ac.uk/fsl/fslwiki/>). HARDI images were first corrected for  
39 motion and eddy current artefacts using *eddy\_correct*, after which vectors were  
40 reoriented using *fdt\_rotate\_bvecs* (Graham, Drobnyak & Zhang, 2016). Then, a brain  
41 mask was created from the corrected b0 image using *fsroi* and skull-stripped using  
42 *bet* (Smith, 2002). Tensors were fitted using *dwi2tensor*, and fractional anisotropy  
43 (FA) values were computed for each voxel using *tensor2metric* (Veraart et al., 2013).  
44 Next, the DWI response function was estimated using *dwi2response* and the fiber

1 orientation distribution (FOD), which was derived using constrained spherical  
2 deconvolution (CSD) with harmonic order 8 as implemented in *dwi2fod* (Tournier et  
3 al., 2004, 2007).  
4  
5

6  
7 For tractography, each individual's T1-weighted image was first segmented  
8 using FSL's *first* to derive individual masks for gray matter and cerebro-spinal fluid  
9 (CSF; Patenaude et al., 2011). Then, masks for left and right amygdala, as well as left  
10 and right fusiform gyrus were defined as anatomical regions of interest using the AAL  
11 atlas and masked using individual gray matter masks (Tzourio-Mazoyer et al., 2002).  
12 All masks were transformed into individual diffusion space using *flirt* (Jenkinson &  
13 Smith, 2001; Jenkinson et al., 2002). Unidirectional probabilistic streamlines between  
14 amygdala seed masks and fusiform gyrus inclusion masks were computed for each  
15 hemisphere using *tckgen*, the FODs derived from CSD, an exclusion mask derived  
16 from each individual's CSF, and the iFOD2 algorithm with a step size of 1.15 and a  
17 cut-off of 0.15 (Tournier et al., 2010, 2012). After visual inspection, streamlines were  
18 converted to track-density images with *tckmap*, thresholded using *mrthreshold*,  
19 binarized with *fslmaths*, and used as masks to extract the mean values for each  
20 individual from the FA images using *fslstats* (Calamante et al., 2010).  
21  
22  
23  
24  
25  
26  
27  
28  
29  
30  
31  
32  
33  
34  
35  
36  
37  
38  
39  
40  
41  
42  
43

#### 44 *2.6 Structure-Function-Behaviour Analysis*

45  
46 To assess the **relation** between reaction time, ILF FA values, and amygdala  
47 functional connectivity, average time-courses of seed regions in left and right dorsal  
48 amygdala were first extracted from each individual using a 5-mm sphere centered at  
49 MNI coordinates [-20 -8 -12] and [22 -6 -12]. The coordinates were chosen based on  
50 a priori anatomical information about the location of the left and right amygdala as  
51 well as the results of the whole-brain analysis, where the coordinates represent peak  
52  
53  
54  
55  
56  
57  
58  
59  
60  
61  
62  
63  
64  
65

1 amygdala activations differentiating the processing of fearful and angry faces from  
2 shapes. Then, the mean reaction times, mean ILF FA values, and functional seed  
3 values were correlated with each participant's whole-brain activity and submitted to  
4  
5  
6  
7 **seed** PLS analysis (Krishnan et al., 2011). **In seed** PLS analysis, the results **display** the  
8  
9 Pearson product-moment correlation coefficient between brain scores of the LV and  
10  
11 the reaction times, ILF FA values, and amygdala functional seed values for each  
12  
13 condition (Marstaller et al., 2015). As a consequence, these correlations reflect  
14  
15 individual differences in the three-way **relation between structure, function, and**  
16  
17  
18  
19 **behavior.**  
20  
21  
22  
23

### 24 **3. Results**

#### 25 *3.1 Reaction times*

26  
27 Repeated measures two-sided t-tests revealed that participants responded  
28  
29 significantly faster to shapes (mean RT = 899.14 ms, SD = 163.89 ms) than angry  
30  
31 (mean RT = 1096.11 ms, SD = 170.78 ms;  $t(27) = 6.3$ ,  $p < 0.001$ ) and fearful faces  
32  
33 (mean RT = 1065.88 ms, SD = 153.61 ms;  $t(27) = 5.8$ ,  $p < 0.001$ ). There was no  
34  
35 significant difference in reaction times between angry and fearful faces ( $t(27) = 1.3$ ,  $p$   
36  
37 = 0.21; see Figure 1A). Reaction times for angry and fearful faces were highly  
38  
39 correlated ( $r = 0.7$ ).  
40  
41  
42  
43  
44  
45  
46  
47

#### 48 *3.2 ILF white-matter integrity*

49  
50 Group-mean FA-values were 0.42 (SD = 0.03) for the left and 0.41 (SD =  
51  
52 0.06) for the right ILF. A two-sided repeated measures t-test showed no significant  
53  
54 differences between the two hemispheres ( $t(27) = 1.5$ ,  $p = 0.13$ ; see Figure 1B).  
55  
56  
57  
58  
59  
60  
61  
62  
63  
64  
65

(INSERT FIGURE 1 HERE)

### 3.3 *Whole-brain task-related functional activity*

PLS analysis resulted in two significant whole-brain activity patterns. The first pattern of activity differentiated the control condition (shapes) from face presentations and demonstrated a shared activation pattern for angry and fearful expressions. Angry and fearful faces were associated with increased activity in the core and extended emotional face processing system, including bilateral inferior occipital gyrus, fusiform gyrus, and dorsal amygdala (see cool colours in Figure 2). Presentation of shapes resulted in greater activity in posterior parietal cortices (see warm colours in Figure 2; see Table 1).

(INSERT FIGURE 2 HERE)

The second significant pattern of activity differentiated angry from fearful faces. For angry faces, the pattern showed increased activity in the right orbitofrontal cortex, left caudate nucleus, and middle frontal cortex, as well as in areas commonly associated with semantic processing (right hippocampus and middle temporal gyrus; Binder et al., 2009), salience detection (anterior cingulate cortex; Critchley, 2005), and bottom-up attention (right ventrolateral prefrontal cortex and right supramarginal gyrus; Fox et al., 2006; see warm colours in Figure 3). For fearful faces, the pattern showed increased activity in the right ventral amygdala, fusiform gyrus, and left pallidum (see cool colours in Figure 3; see Table 2).

(INSERT FIGURE 3 HERE)

1  
2  
3  
4  
5 *3.4 Three-way relation between reaction time, ILF integrity, and amygdala functional*  
6  
7 *connectivity*

8  
9  
10 PLS analysis revealed two significant whole-brain patterns of amygdala  
11 functional connectivity that showed a different relation between functional  
12 connectivity, behaviour and ILF white matter integrity for angry and fearful faces.  
13  
14 During perception of angry facial expressions, a set of limbic-temporal regions was  
15 functionally connected to the right ( $r = 0.37$ ) but not the left amygdala ( $r = -0.028$ ).  
16  
17 This functional network was negatively correlated with reaction times ( $r = -0.72$ ), but  
18 positively correlated with FA values of the left ( $r = 0.45$ ) and right ILF ( $r = 0.37$ ) and  
19 included bilateral hippocampus, brainstem, and the right temporal pole (see Figure 4).  
20  
21 These results therefore show that individuals, who were faster at identifying angry  
22 faces, engaged this extended amygdala network more strongly, had better  
23 connectivity with the right amygdala, and a higher ILF white matter integrity  
24 bilaterally. Individual differences in the three-way relation between behaviour, white  
25 matter integrity, and functional connectivity are displayed as scatter plots that indicate  
26 how much each factor correlated with the depicted pattern of activity across the  
27 sample (see Figure 4).  
28  
29  
30  
31  
32  
33  
34  
35  
36  
37  
38  
39  
40  
41  
42  
43  
44  
45  
46  
47  
48  
49  
50  
51  
52  
53  
54  
55  
56  
57  
58  
59  
60  
61  
62  
63  
64  
65

(INSERT FIGURE 4 HERE)

66  
67  
68  
69  
70  
71  
72  
73  
74  
75  
76  
77  
78  
79  
80  
81  
82  
83  
84  
85  
86  
87  
88  
89  
90  
91  
92  
93  
94  
95  
96  
97  
98  
99  
100  
101  
102  
103  
104  
105  
106  
107  
108  
109  
110  
111  
112  
113  
114  
115  
116  
117  
118  
119  
120  
121  
122  
123  
124  
125  
126  
127  
128  
129  
130  
131  
132  
133  
134  
135  
136  
137  
138  
139  
140  
141  
142  
143  
144  
145  
146  
147  
148  
149  
150  
151  
152  
153  
154  
155  
156  
157  
158  
159  
160  
161  
162  
163  
164  
165  
166  
167  
168  
169  
170  
171  
172  
173  
174  
175  
176  
177  
178  
179  
180  
181  
182  
183  
184  
185  
186  
187  
188  
189  
190  
191  
192  
193  
194  
195  
196  
197  
198  
199  
200  
201  
202  
203  
204  
205  
206  
207  
208  
209  
210  
211  
212  
213  
214  
215  
216  
217  
218  
219  
220  
221  
222  
223  
224  
225  
226  
227  
228  
229  
230  
231  
232  
233  
234  
235  
236  
237  
238  
239  
240  
241  
242  
243  
244  
245  
246  
247  
248  
249  
250  
251  
252  
253  
254  
255  
256  
257  
258  
259  
260  
261  
262  
263  
264  
265  
266  
267  
268  
269  
270  
271  
272  
273  
274  
275  
276  
277  
278  
279  
280  
281  
282  
283  
284  
285  
286  
287  
288  
289  
290  
291  
292  
293  
294  
295  
296  
297  
298  
299  
300  
301  
302  
303  
304  
305  
306  
307  
308  
309  
310  
311  
312  
313  
314  
315  
316  
317  
318  
319  
320  
321  
322  
323  
324  
325  
326  
327  
328  
329  
330  
331  
332  
333  
334  
335  
336  
337  
338  
339  
340  
341  
342  
343  
344  
345  
346  
347  
348  
349  
350  
351  
352  
353  
354  
355  
356  
357  
358  
359  
360  
361  
362  
363  
364  
365  
366  
367  
368  
369  
370  
371  
372  
373  
374  
375  
376  
377  
378  
379  
380  
381  
382  
383  
384  
385  
386  
387  
388  
389  
390  
391  
392  
393  
394  
395  
396  
397  
398  
399  
400  
401  
402  
403  
404  
405  
406  
407  
408  
409  
410  
411  
412  
413  
414  
415  
416  
417  
418  
419  
420  
421  
422  
423  
424  
425  
426  
427  
428  
429  
430  
431  
432  
433  
434  
435  
436  
437  
438  
439  
440  
441  
442  
443  
444  
445  
446  
447  
448  
449  
450  
451  
452  
453  
454  
455  
456  
457  
458  
459  
460  
461  
462  
463  
464  
465  
466  
467  
468  
469  
470  
471  
472  
473  
474  
475  
476  
477  
478  
479  
480  
481  
482  
483  
484  
485  
486  
487  
488  
489  
490  
491  
492  
493  
494  
495  
496  
497  
498  
499  
500  
501  
502  
503  
504  
505  
506  
507  
508  
509  
510  
511  
512  
513  
514  
515  
516  
517  
518  
519  
520  
521  
522  
523  
524  
525  
526  
527  
528  
529  
530  
531  
532  
533  
534  
535  
536  
537  
538  
539  
540  
541  
542  
543  
544  
545  
546  
547  
548  
549  
550  
551  
552  
553  
554  
555  
556  
557  
558  
559  
560  
561  
562  
563  
564  
565  
566  
567  
568  
569  
570  
571  
572  
573  
574  
575  
576  
577  
578  
579  
580  
581  
582  
583  
584  
585  
586  
587  
588  
589  
590  
591  
592  
593  
594  
595  
596  
597  
598  
599  
600  
601  
602  
603  
604  
605  
606  
607  
608  
609  
610  
611  
612  
613  
614  
615  
616  
617  
618  
619  
620  
621  
622  
623  
624  
625  
626  
627  
628  
629  
630  
631  
632  
633  
634  
635  
636  
637  
638  
639  
640  
641  
642  
643  
644  
645  
646  
647  
648  
649  
650  
651  
652  
653  
654  
655  
656  
657  
658  
659  
660  
661  
662  
663  
664  
665  
666  
667  
668  
669  
670  
671  
672  
673  
674  
675  
676  
677  
678  
679  
680  
681  
682  
683  
684  
685  
686  
687  
688  
689  
690  
691  
692  
693  
694  
695  
696  
697  
698  
699  
700  
701  
702  
703  
704  
705  
706  
707  
708  
709  
710  
711  
712  
713  
714  
715  
716  
717  
718  
719  
720  
721  
722  
723  
724  
725  
726  
727  
728  
729  
730  
731  
732  
733  
734  
735  
736  
737  
738  
739  
740  
741  
742  
743  
744  
745  
746  
747  
748  
749  
750  
751  
752  
753  
754  
755  
756  
757  
758  
759  
760  
761  
762  
763  
764  
765  
766  
767  
768  
769  
770  
771  
772  
773  
774  
775  
776  
777  
778  
779  
780  
781  
782  
783  
784  
785  
786  
787  
788  
789  
790  
791  
792  
793  
794  
795  
796  
797  
798  
799  
800  
801  
802  
803  
804  
805  
806  
807  
808  
809  
810  
811  
812  
813  
814  
815  
816  
817  
818  
819  
820  
821  
822  
823  
824  
825  
826  
827  
828  
829  
830  
831  
832  
833  
834  
835  
836  
837  
838  
839  
840  
841  
842  
843  
844  
845  
846  
847  
848  
849  
850  
851  
852  
853  
854  
855  
856  
857  
858  
859  
860  
861  
862  
863  
864  
865  
866  
867  
868  
869  
870  
871  
872  
873  
874  
875  
876  
877  
878  
879  
880  
881  
882  
883  
884  
885  
886  
887  
888  
889  
890  
891  
892  
893  
894  
895  
896  
897  
898  
899  
900  
901  
902  
903  
904  
905  
906  
907  
908  
909  
910  
911  
912  
913  
914  
915  
916  
917  
918  
919  
920  
921  
922  
923  
924  
925  
926  
927  
928  
929  
930  
931  
932  
933  
934  
935  
936  
937  
938  
939  
940  
941  
942  
943  
944  
945  
946  
947  
948  
949  
950  
951  
952  
953  
954  
955  
956  
957  
958  
959  
960  
961  
962  
963  
964  
965  
966  
967  
968  
969  
970  
971  
972  
973  
974  
975  
976  
977  
978  
979  
980  
981  
982  
983  
984  
985  
986  
987  
988  
989  
990  
991  
992  
993  
994  
995  
996  
997  
998  
999  
1000

1 negatively correlated with reaction time ( $r = -0.37$ ) but positively with FA values of  
2 the left ( $r = 0.3$ ) and right ILF ( $r = 0.51$ ) and included bilateral lingual gyrus,  
3  
4 precuneus, middle and superior frontal gyrus, supramarginal gyrus, and precentral  
5  
6 gyrus meaning that individuals, who were faster at differentiating fearful faces,  
7  
8 engaged this fronto-parietal-occipital network more strongly, had lower connectivity  
9  
10 with the right amygdala, and a higher ILF white matter integrity bilaterally. Individual  
11  
12 differences in the three-way **relation** between behaviour, white matter integrity, and  
13  
14 functional connectivity are displayed as scatter plots that indicate how much each  
15  
16 factor correlated with the depicted pattern of activity across the sample (see Figure 5).  
17  
18  
19  
20  
21  
22  
23

24 (INSERT FIGURE 5 HERE)  
25  
26  
27  
28

## 29 **5. Discussion**

30  
31 In social interactions, individuals who are slower at distinguishing between  
32  
33 facial expressions signalling direct and indirect threat might be at a serious  
34  
35 disadvantage. However, the neurobiological underpinnings of individual differences  
36  
37 in face processing are not yet fully understood. The aim of this study was to  
38  
39 investigate how the speed of emotion recognition is related to the structural and  
40  
41 functional connectivity underlying the differentiation of direct and indirect threat  
42  
43 displays. The analysis of the three-way **relation** between behaviour, structure, and  
44  
45 function underlying the core and extended systems for angry and fearful face  
46  
47 processing revealed behaviourally relevant individual differences. Individuals who  
48  
49 were faster at identifying angry faces engaged areas of the extended emotional system  
50  
51 more strongly than individuals with slower reaction times. These faster individuals  
52  
53 further showed higher white matter integrity in the ILF and stronger functional  
54  
55  
56  
57  
58  
59  
60  
61  
62  
63  
64  
65

1 connectivity with the right amygdala, suggesting that an efficient structural and  
2 functional connectivity between the core and extended emotional systems is crucial  
3 for the rapid processing of facial expressions signalling direct threat. This finding  
4 implicates that the high survival value of rapid and appropriate responses to direct  
5 threat has a defined neurobiological correlate.  
6  
7  
8  
9  
10

11 With respect to fearful faces that signal indirect threat, our results showed that  
12 individuals who were faster at discriminating fearful faces also had more intact white  
13 matter in the ILF but less functional connectivity between the face processing  
14 network and the amygdala. Those faster individuals engaged more regions outside of  
15 the face processing network related to attention and visual processing, suggesting that  
16 the processing speed of facial expressions signalling indirect threat profits from the  
17 recruitment of additional visual-attentional systems, which are engaged in searching  
18 for novel cues that help reduce the ambiguity associated with indirect threat  
19 expressions (Whalen et al., 2001; Phelps, Ling, & Carrasco, 2005). In contrast to  
20 direct threat, the rapid recognition of indirect threat, therefore, seems to depend less  
21 on the cortical face-processing network and instead might rely more on a subcortical  
22 pathway (Villeumier et al., 2003). In addition, individual differences in the rapid  
23 recognition of indirect threat displays seem to directly translate into the ability to  
24 gather additional information that reduces the ambiguity associated with fearful facial  
25 expressions, and individuals who rapidly reduce ambiguity might profit from higher  
26 white matter integrity in the ILF along the ventral visual stream.  
27  
28  
29  
30  
31  
32  
33  
34  
35  
36  
37  
38  
39  
40  
41  
42  
43  
44  
45  
46  
47  
48  
49  
50

51 The whole-brain results confirm previous findings by demonstrating the  
52 engagement of the core face-processing network, which consists of inferior occipital  
53 and fusiform gyrus and the extended emotional system centered around the amygdala,  
54 for both angry and fearful faces (Adolphs, 2002; Haxby et al. 2002; LaBar et al.,  
55  
56  
57  
58  
59  
60  
61  
62  
63  
64  
65



2003; Gobbini & Haxby, 2007). The results further show that the dorsal amygdala and fusiform gyrus are engaged during the perception of both angry and fearful faces, which is in accordance with previous findings demonstrating increased vigilance during perception of threat (Davis & Whalen, 2001; Williams et al., 2001). The absence of activity in the superior temporal sulcus and premotor cortices in our data is possibly related to the static stimuli used in this experiment (Grèzes, Pichon & de Gelder, 2007; Said, Haxby & Todorov, 2011). Perception of angry faces additionally activated cortical regions associated with evaluative processing, such as the salience (Menon & Uddin, 2010; Pichon, de Gelder & Grèzes, 2012) and ventral attention networks (Corbetta & Shulman, 2002), as well as regions associated with memory processing (Haxby et al., 1996; Frey & Petrides, 2003; Tsukiura & Cabeza, 2008). This finding suggests that angry faces might engage cortical regions related to evaluative, contextual processing more strongly than fearful faces, perhaps because anger directs attention towards the angry individual, whereas fear directs attention towards the ambiguous cause of the threat (Grosbras & Paus, 2006; Pichon, de Gelder & Grèzes, 2009). Fearful faces additionally engaged the amygdala and fusiform gyrus, which is in line with previous findings and suggests increased processing of fearful compared to angry facial expressions within regions of the core and extended emotional faces processing systems (Whalen et al., 2001). Perception of fearful faces further engaged the left globus pallidum, which might be related to the initiation of a fight-or-flight response (Korzeniewska, Kasicki & Zagrodzka, 1997; Grèzes & Dezeccache, 2014).

In sum, our results extend our current knowledge about the networks involved in the processing of emotional facial expressions by demonstrating that individual differences in the structural and functional connectivity within and between the core

1 and extended emotional face-processing systems affect the speed at which emotional  
2 faces are discriminated. The associated adaptive value of efficient structural and  
3 functional connectivity between the core and extended emotional face-processing  
4 systems points towards a neurobiological cause for individual differences in social  
5 interactions. As a consequence, genetic and environmental factors that influence the  
6 development and age-related degeneration of structural and functional connectivity  
7 underlying emotional face discrimination might determine an individual's success in  
8 responding to threat in social interactions and hence impart a high survival value  
9 (Cohen Kadosh, 2011; Scherf et al., 2014; Shaw et al., 2016).  
10  
11  
12  
13  
14  
15  
16  
17  
18  
19  
20  
21  
22  
23

### 24 **Acknowledgements**

25  
26 This work was funded by the Australian Research Council Special Research  
27 Initiative: Science of Learning Research Centre (project number SR120300015).  
28  
29  
30  
31  
32  
33  
34  
35  
36  
37  
38  
39  
40  
41  
42  
43  
44  
45  
46  
47  
48  
49  
50  
51  
52  
53  
54  
55  
56  
57  
58  
59  
60  
61  
62  
63  
64  
65

**References**

- 1  
2 Adolphs R (2002) Recognizing emotion from facial expressions: psychological and  
3  
4  
5 neurological mechanisms. *Behav Cogn Neurosci Rev.* 1: 21-62.  
6
- 7 Amaral DG, Behniea H, Kelly JL (2003) Topographic organization of projections  
8  
9  
10 from the amygdala to the visual cortex in the macaque monkey. *Neuroscience.*  
11  
12 118: 1099-120.  
13
- 14 Bannerman RL, Milders M, de Gelder B, Sahraie A (2009) Orienting to threat: faster  
15  
16  
17 localization of fearful facial expressions and body postures revealed by saccadic  
18  
19  
20 eye movements. *Proc Biol Sci.* 276: 1635-41.  
21
- 22 Binder JR, Desai RH, Graves WW, Conant LL (2009) Where is the semantic system?  
23  
24  
25 A critical review and meta-analysis of 120 functional neuroimaging studies.  
26  
27  
28 *Cereb Cortex.* 19: 2767-96.  
29
- 30 Calamante F, Tournier JD, Jackson GD, Connelly A (2010) Track-density imaging  
31  
32  
33 (TDI): super-resolution white matter imaging using whole-brain track-density  
34  
35  
36 mapping. *Neuroimage.* 53: 1233-43.  
37
- 38 Catani M, Jones DK, Donato R, Ffytche DH (2003) Occipito-temporal connections in  
39  
40  
41 the human brain. *Brain.* 126: 2093-107.  
42
- 43 Cisek P, Kalaska JF (2010) Neural mechanisms for interacting with a world full of  
44  
45  
46 action choices. *Annu Rev Neurosci.* 33: 269-98.  
47
- 48 Cohen Kadosh K (2011) What can emerging cortical face networks tell us about  
49  
50  
51 mature brain organisation? *Dev Cogn Neurosci.* 1: 246-55.  
52
- 53 Corbetta M, Shulman GL (2002) Control of goal-directed and stimulus-driven  
54  
55  
56 attention in the brain. *Nat Rev Neurosci.* 3: 201-15.  
57
- 58 Critchley HD (2005) Neural mechanisms of autonomic, affective, and cognitive  
59  
60  
61  
62  
63  
64  
65 integration. *Journal of Comparative Neurology.* 493: 154-66.

- 1  
2  
3  
4  
5  
6  
7  
8  
9  
10  
11  
12  
13  
14  
15  
16  
17  
18  
19  
20  
21  
22  
23  
24  
25  
26  
27  
28  
29  
30  
31  
32  
33  
34  
35  
36  
37  
38  
39  
40  
41  
42  
43  
44  
45  
46  
47  
48  
49  
50  
51  
52  
53  
54  
55  
56  
57  
58  
59  
60  
61  
62  
63  
64  
65
- de Gelder B, Terburg D, Morgan B, Hortensius R, Stein DJ, van Honk J (2014) The role of human basolateral amygdala in ambiguous social threat perception. *Cortex*. 52: 28-34.
- De Sonnevile LM, Verschoor CA, Njikiktjien C, Op het Veld V, Toorenaar N, Vranken M (2002) Facial identity and facial emotions: speed, accuracy, and processing strategies in children and adults. *J Clin Exp Neuropsychol*. 24: 200-13.
- Fox MD, Corbetta M, Snyder AZ, Vincent JL, Raichle ME (2006) Spontaneous neuronal activity distinguishes human dorsal and ventral attention systems. *Proc Natl Acad Sci*. 103: 10046-51.
- Frey S, Petrides M (2003) Greater orbitofrontal activity predicts better memory for faces. *Eur J Neurosci*. 17: 2755-8.
- Gobbini MI, Haxby JV (2007) Neural systems for recognition of familiar faces. *Neuropsychologia*. 45: 32-41.
- Graham MS, Drobnyak I, Zhang H (2016) Realistic simulation of artefacts in diffusion MRI for validating post-processing correction techniques. *Neuroimage*. 125: 1079-94.
- Grèzes J, Dezeache G (2014) How do shared-representations and emotional processes cooperate in response to social threat signals? *Neuropsychologia*. 55: 105-14.
- Grèzes J, Pichon S, de Gelder B (2007) Perceiving fear in dynamic body expressions. *Neuroimage*. 35: 959-67.
- Grosbras MH, Paus T (2006) Brain networks involved in viewing angry hands or faces. *Cereb Cortex*. 16: 1087-96.

- 1  
2  
3  
4  
5  
6  
7  
8  
9  
10  
11  
12  
13  
14  
15  
16  
17  
18  
19  
20  
21  
22  
23  
24  
25  
26  
27  
28  
29  
30  
31  
32  
33  
34  
35  
36  
37  
38  
39  
40  
41  
42  
43  
44  
45  
46  
47  
48  
49  
50  
51  
52  
53  
54  
55  
56  
57  
58  
59  
60  
61  
62  
63  
64  
65
- Hansen CH, Hansen RD (1988) Finding the face in the crowd: an anger superiority effect. *J Pers Soc Psychol.* 54: 917-24.
- Hariri AR, Bookheimer SY, Mazziotta JC (2000) Modulating emotional responses: effects of a neocortical network on the limbic system. *Neuroreport.* 11:43-8.
- Haxby JV, Hoffman EA, Gobbini MI (2002) Human neural systems for face recognition and social communication. *Biol Psychiatry.* 51: 59-67.
- Haxby JV, Ungerleider LG, Horwitz B, Maisog JM, Rapoport SI, Grady CL (1996) Face encoding and recognition in the human brain. *Proc Natl Acad Sci.* 93: 922-7.
- Herrington JD, Taylor JM, Grupe DW, Curby KM, Schultz RT (2011) Bidirectional communication between amygdala and fusiform gyrus during facial recognition. *Neuroimage.* 56: 2348-55.
- Jenkinson M, Smith S (2001) A global optimisation method for robust affine registration of brain images. *Med Image Anal.* 5: 143-56.
- Jenkinson M, Bannister P, Brady M, Smith S (2002) Improved optimization for the robust and accurate linear registration and motion correction of brain images. *Neuroimage.* 17: 825-41.
- Kleinhans NM, Richards T, Sterling L, Stegbauer KC, Mahurin R, Johnson LC, Greenson J, Dawson G, Aylward E (2008) Abnormal functional connectivity in autism spectrum disorders during face processing. *Brain.* 131: 1000-12.
- Koldewyn K, Yendiki A, Weigelt S, Gweon H, Julian J, Richardson H, Malloy C, Saxe R, Fischl B, Kanwisher N (2014) Differences in the right inferior longitudinal fasciculus but no general disruption of white matter tracts in children with autism spectrum disorder. *Proc Natl Acad Sci USA.* 111: 1981-6.

- 1  
2  
3  
4  
5  
6  
7  
8  
9  
10  
11  
12  
13  
14  
15  
16  
17  
18  
19  
20  
21  
22  
23  
24  
25  
26  
27  
28  
29  
30  
31  
32  
33  
34  
35  
36  
37  
38  
39  
40  
41  
42  
43  
44  
45  
46  
47  
48  
49  
50  
51  
52  
53  
54  
55  
56  
57  
58  
59  
60  
61  
62  
63  
64  
65
- Korzeniewska A, Kasicki S, Zagrodzka J (1997) Electrophysiological correlates of the limbic-motor interactions in various behavioral states in rats. *Behav Brain Res.* 87: 69-83.
- Krishnan A, Williams LJ, McIntosh AR, Abdi H (2011) Partial Least Squares (PLS) methods for neuroimaging: a tutorial and review. *Neuroimage.* 56: 455-75.
- LaBar KS, Crupain MJ, Voyvodic JT, McCarthy G (2003) Dynamic perception of facial affect and identity in the human brain. *Cereb Cortex.* 13: 1023-33.
- Langner O, Dotsch R, Bijlstra G, Wigboldus DHJ, Hawk ST, van Knippenberg A (2010). Presentation and validation of the Radboud Faces Database. *Cognition & Emotion.* 24: 1377-88.
- Lo LY, Cheng MY (2015) A quick eye to anger: An investigation of a differential effect of facial features in detecting angry and happy expressions. *Int J Psychol.* doi: 10.1002/ijop.12202. [Epub ahead of print].
- Marstaller L, Williams M, Rich A, Savage G, Burianová H (2015) Aging and large-scale functional networks: white matter integrity, gray matter volume, and functional connectivity in the resting state. *Neuroscience.* 290: 369-78.
- McIntosh AR, Bookstein FL, Haxby JV, Grady CL (1996). Spatial pattern analysis of functional brain images using partial least squares. *Neuroimage*, 3(3), 143-157.
- McIntosh AR, Chau WK, Protzner AB (2004). Spatiotemporal analysis of event-related fMRI data using partial least squares. *Neuroimage*, 23(2), 764-775.
- Menon V, Uddin LQ (2010) Saliency, switching, attention and control: a network model of insula function. *Brain Struct Funct.* 214: 655-67.
- Ogawa S, Lee TM, Kay AR, Tank DW (1990). Brain magnetic resonance imaging with contrast dependent on blood oxygenation. *Proc Natl Acad Sci.* 87: 9868-72.

- 1 Patenaude B, Smith SM, Kennedy D, Jenkinson M (2011) A Bayesian model of shape  
2 and appearance for subcortical brain. *NeuroImage*. 56: 907-922.  
3  
4 Phelps EA, LeDoux JE (2005) Contributions of the amygdala to emotion processing:  
5 from animal models to human behavior. *Neuron*. 48: 175-87.  
6  
7 Phelps EA, Ling S, Carrasco M (2006) Emotion facilitates perception and potentiates  
8 the perceptual benefits of attention. *Psychol Sci*. 17: 292-9.  
9  
10 Pichon S, de Gelder B, Grèzes J (2009) Two different faces of threat. Comparing the  
11 neural systems for recognizing fear and anger in dynamic body expressions.  
12 *Neuroimage*. 47: 1873-83.  
13  
14 Pichon S, de Gelder B, Grèzes J (2012) Threat prompts defensive brain responses  
15 independently of attentional control. *Cereb Cortex*. 22: 274-85.  
16  
17 Rossion B, Caldara R, Seghier M, Schuller AM, Lazeyras F, Mayer E (2003) A  
18 network of occipito-temporal face-sensitive areas besides the right middle  
19 fusiform gyrus is necessary for normal face processing. *Brain*. 126: 2381-95.  
20  
21 Said CP, Haxby JV, Todorov A (2011) Brain systems for assessing the affective value  
22 of faces. *Philos Trans R Soc Lond B Biol Sci*. 366: 1660-70.  
23  
24 Scherf KS, Thomas C, Doyle J, Behrmann M (2014) Emerging Structure–Function  
25 Relations in the Developing Face Processing System. *Cereb. Cortex*. 24(11):  
26 2964-80.  
27  
28 Shaw DJ, Mareček R, Grosbras MH, Leonard G, Bruce Pike G, Paus T (2016) Co-  
29 ordinated structural and functional covariance in the adolescent brain underlies  
30 face processing performance. *Soc Cogn Affect Neurosci*. 11: 556-68.  
31  
32 Smith SM (2002) Fast robust automated brain extraction. *Hum Brain Mapp*. 17: 143-  
33 55.  
34  
35  
36  
37  
38  
39  
40  
41  
42  
43  
44  
45  
46  
47  
48  
49  
50  
51  
52  
53  
54  
55  
56  
57  
58  
59  
60  
61  
62  
63  
64  
65

- 1  
2  
3  
4  
5  
6  
7  
8  
9  
10  
11  
12  
13  
14  
15  
16  
17  
18  
19  
20  
21  
22  
23  
24  
25  
26  
27  
28  
29  
30  
31  
32  
33  
34  
35  
36  
37  
38  
39  
40  
41  
42  
43  
44  
45  
46  
47  
48  
49  
50  
51  
52  
53  
54  
55  
56  
57  
58  
59  
60  
61  
62  
63  
64  
65
- Thomas C, Avidan G, Humphreys K, Jung KJ, Gao F, Behrmann M (2009) Reduced structural connectivity in ventral visual cortex in congenital prosopagnosia. *Nat Neurosci.* 12: 29-31.
- Tournier JD, Calamante F, Gadian DG, Connelly A (2004) Direct estimation of the fiber orientation density function from diffusion-weighted MRI data using spherical deconvolution. *Neuroimage.* 23: 1176-85.
- Tournier JD, Calamante F, Connelly A (2007) Robust determination of the fibre orientation distribution in diffusion MRI: non-negativity constrained super-resolved spherical deconvolution. *Neuroimage.* 35: 1459-72.
- Tournier JD, Calamante F, Connelly A (2010) Improved probabilistic streamlines tractography by 2<sup>nd</sup> order integration of fiber orientation distributions. *Proc. Intl. Soc. Mag. Reson. Med.* 18: 1670.
- Tournier JD, Calamante F, Connelly A (2012) MRtrix: Diffusion tractography in crossing fiber regions. *Int. J. Imaging Syst. Technol.* 22: 53–66.
- Tsukiura T, Cabeza R (2008) Orbitofrontal and hippocampal contributions to memory for face-name associations: the rewarding power of a smile. *Neuropsychologia.* 46: 2310-9.
- Tzourio-Mazoyer N, Landeau B, Papathanassiou D, Crivello F, Etard O, Delcroix N, Mazoyer B, Joliot M (2002) Automated anatomical labeling of activations in SPM using a macroscopic anatomical parcellation of the MNI MRI single-subject brain. *Neuroimage.* 15: 273-89.
- Veraart J, Sijbers J, Sunaert S, Leemans A, Jeurissen B (2013) Weighted linear least squares estimation of diffusion MRI parameters: strengths, limitations, and pitfalls. *NeuroImage.* 81: 335-346.



1 Vuilleumier P, Armony JL, Driver J, Dolan RJ (2003) Distinct spatial frequency  
2 sensitivities for processing faces and emotional expressions. *Nat Neurosci.* 6:  
3 624-31.  
4  
5

6  
7 Wang X, Zhen Z, Song Y, Huang L, Kong X, Liu J (2016) The Hierarchical Structure  
8 of the Face Network Revealed by Its Functional Connectivity Pattern. *J*  
9 *Neurosci.* 36: 890-900.  
10  
11

12  
13 Whalen PJ, Shin LM, McInerney SC, Fischer H, Wright CI, Rauch SL (2001) A  
14 functional MRI study of human amygdala responses to facial expressions of  
15 fear versus anger. *Emotion.* 1: 70-83.  
16  
17

18  
19 Williams LM, Phillips ML, Brammer MJ, Skerrett D, Lagopoulos J, Rennie C,  
20 Bahramali H, Olivieri G, David AS, Peduto A, Gordon E (2001) Arousal  
21 dissociates amygdala and hippocampal fear responses: evidence from  
22 simultaneous fMRI and skin conductance recording. *Neuroimage.* 14: 1070-9.  
23  
24  
25  
26  
27  
28  
29  
30  
31  
32  
33  
34  
35  
36  
37  
38  
39  
40  
41  
42  
43  
44  
45  
46  
47  
48  
49  
50  
51  
52  
53  
54  
55  
56  
57  
58  
59  
60  
61  
62  
63  
64  
65

**Figure Captions:**

1  
2  
3  
4  
5 Figure 1: Behaviour and white matter integrity. A: Mean reaction times (+/- SEM)  
6  
7 show significantly slower responses when matching angry and fearful facial  
8  
9 expressions than when matching shapes. B: Mean fractional anisotropy (FA) values  
10  
11 (+/- SEM) for left and right inferior longitudinal fasciculus (left). Tractography results  
12  
13 from a representative subject (right).  
14  
15  
16  
17  
18

19 Figure 2: Whole-brain activity differentiating faces and shapes. Warm colours show  
20  
21 functional activity in posterior parietal cortices during processing of shapes. Cool  
22  
23 colours depict functional activity in the core and extended emotional face processing  
24  
25 regions, including inferior occipital gyrus, fusiform gyrus, and dorsal amygdala,  
26  
27 during processing of angry and fearful facial expressions.  
28  
29  
30  
31  
32  
33

34 Figure 3: Whole-brain activity contrasting angry and fearful facial expressions. Warm  
35  
36 colours show functional activity related to angry facial expressions. Cool colours  
37  
38 depict functional activity related to fearful facial expressions.  
39  
40  
41  
42

43 Figure 4: Individual differences in the three-way **relation** between behaviour,  
44  
45 functional connectivity, and ILF white matter integrity for angry faces. Left: Whole-  
46  
47 brain patterns showing functional connectivity with the right amygdala negatively  
48  
49 correlated with reaction times and positively with ILF FA values, including  
50  
51 hippocampus, brainstem, and the right temporal pole. Right: Scatter plots demonstrate  
52  
53 correlations between individual PLS brain scores (indicating how strongly each  
54  
55 individual expressed the whole-brain pattern) on the ordinate and the covariates  
56  
57  
58  
59  
60  
61  
62  
63  
64  
65

1 reaction time (in msec), left and right amygdala functional seeds (in % signal change),  
2 as well as mean FA values of left and right ILF (in arbitrary units) on the abscissa.  
3  
4  
5  
6

7 Figure 5: Three-way **relation** between behaviour, functional connectivity, and ILF  
8 white matter integrity for fearful faces. Left: Whole-brain patterns showing functional  
9 connectivity with the right amygdala correlated with reaction times and ILF FA  
10 values, including bilateral lingual gyrus, precuneus, middle and superior frontal gyrus,  
11 supramarginal gyrus, and precentral gyrus. Right: Scatter plots demonstrate  
12 correlations between individual PLS brain scores (indicating how strongly each  
13 individual expressed the whole-brain pattern) on the ordinate and the covariates  
14 reaction time (in msec), left and right amygdala functional seeds (in % signal change),  
15 as well as mean FA values of left and right ILF (in arbitrary units) on the abscissa.  
16  
17  
18  
19  
20  
21  
22  
23  
24  
25  
26  
27  
28  
29  
30  
31  
32  
33  
34  
35  
36  
37  
38  
39  
40  
41  
42  
43  
44  
45  
46  
47  
48  
49  
50  
51  
52  
53  
54  
55  
56  
57  
58  
59  
60  
61  
62  
63  
64  
65

Figure 1  
[Click here to download high resolution image](#)

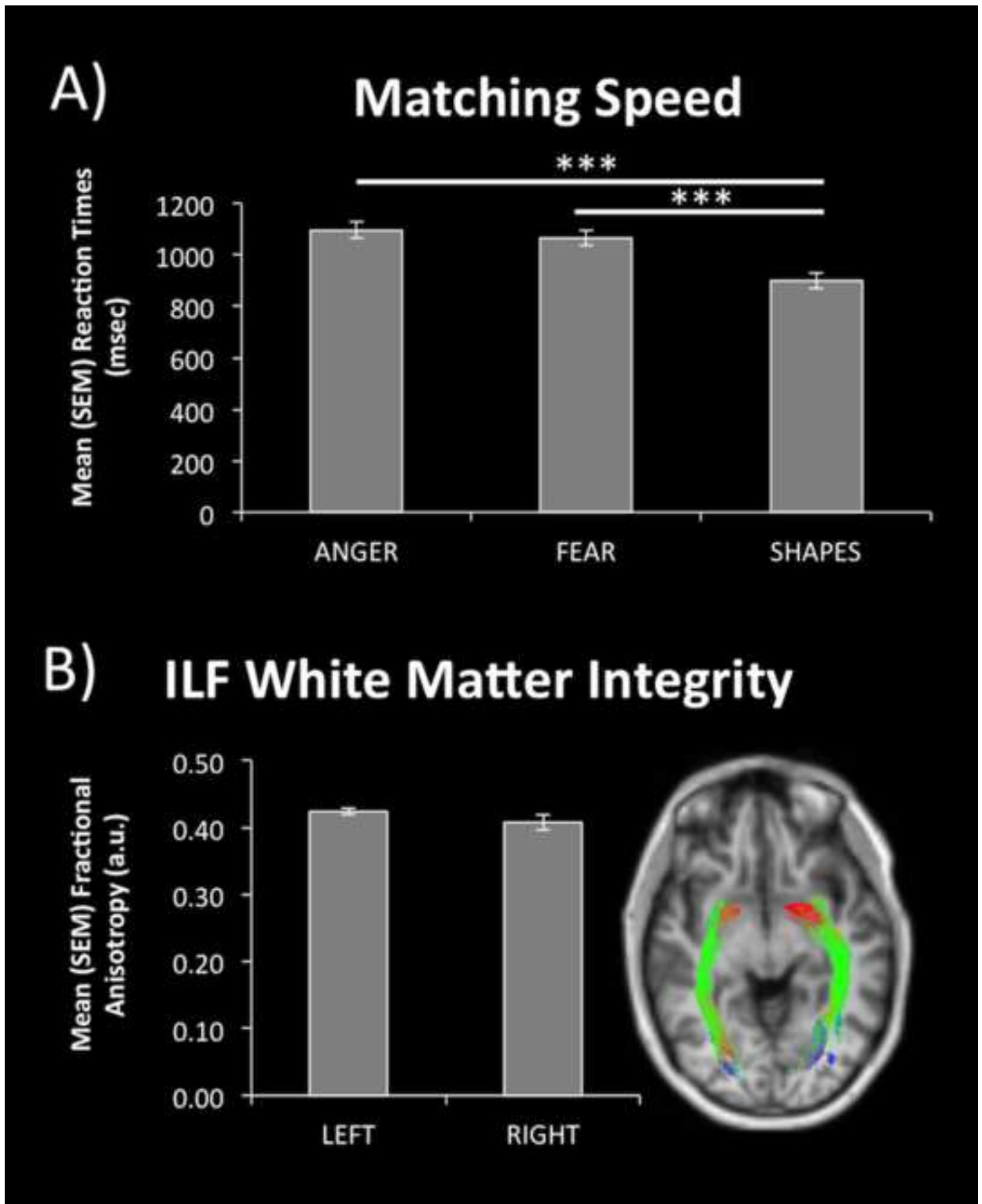


Figure 2  
[Click here to download high resolution image](#)

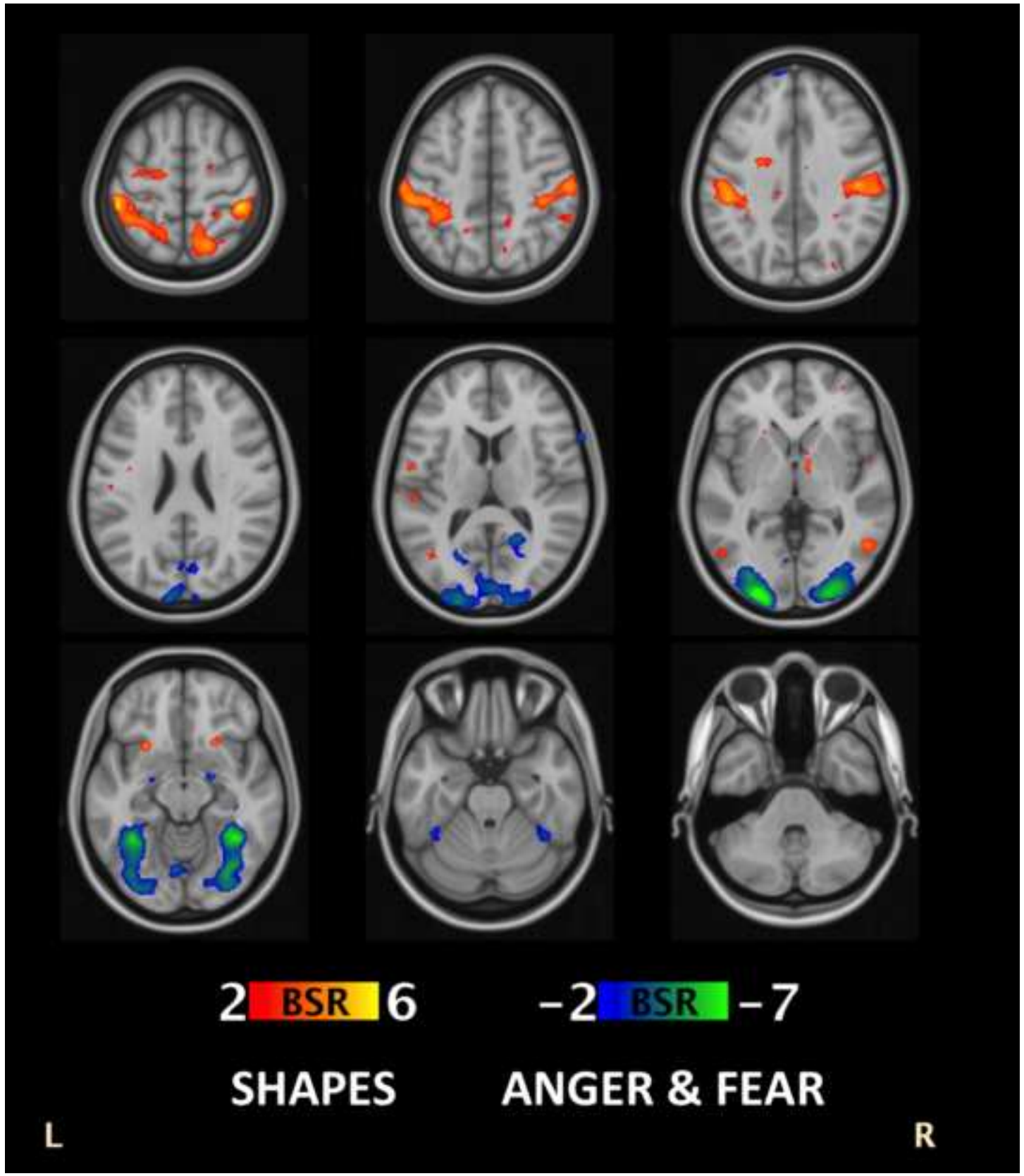


Figure 3  
[Click here to download high resolution image](#)

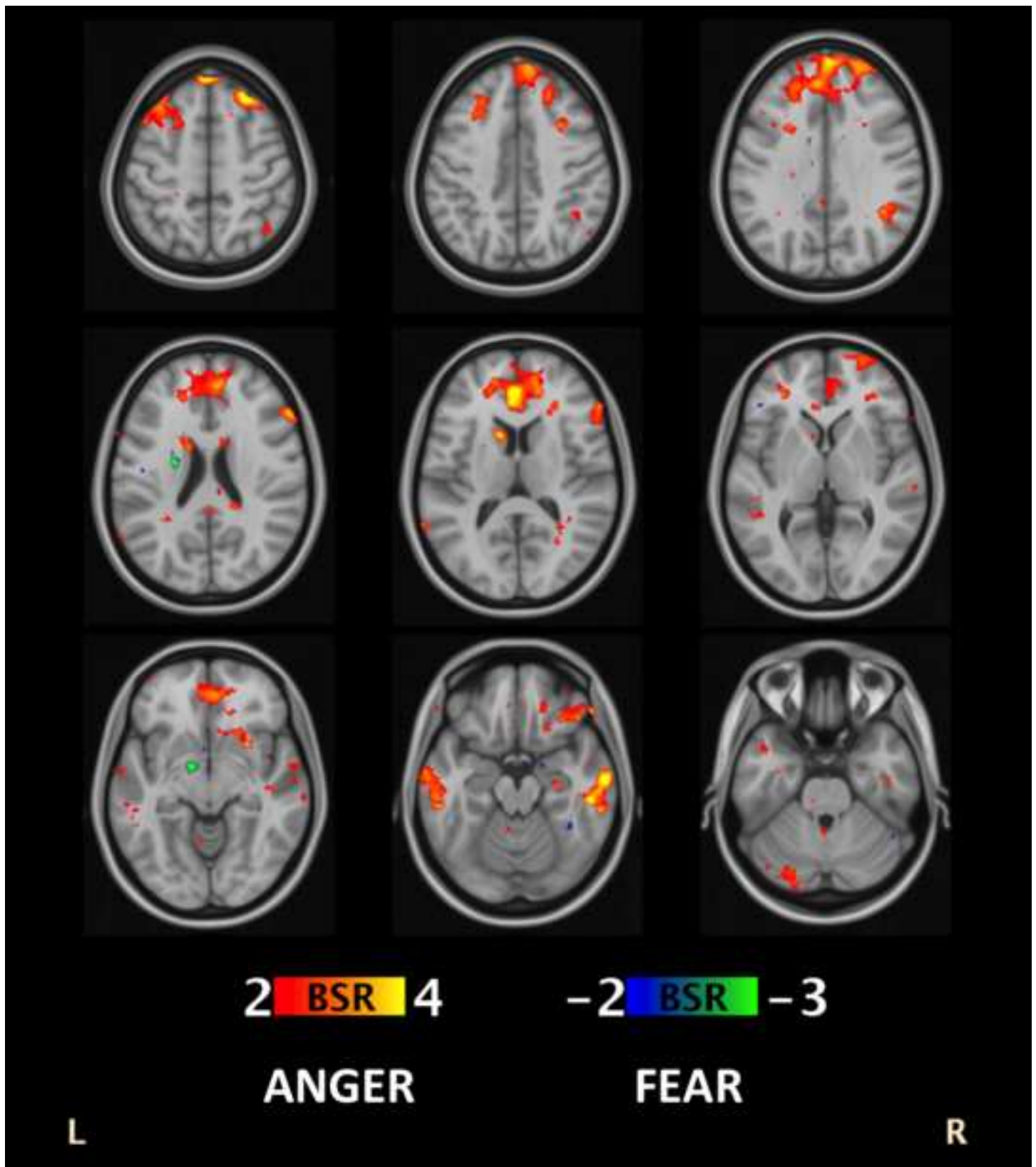


Figure 4  
[Click here to download high resolution image](#)

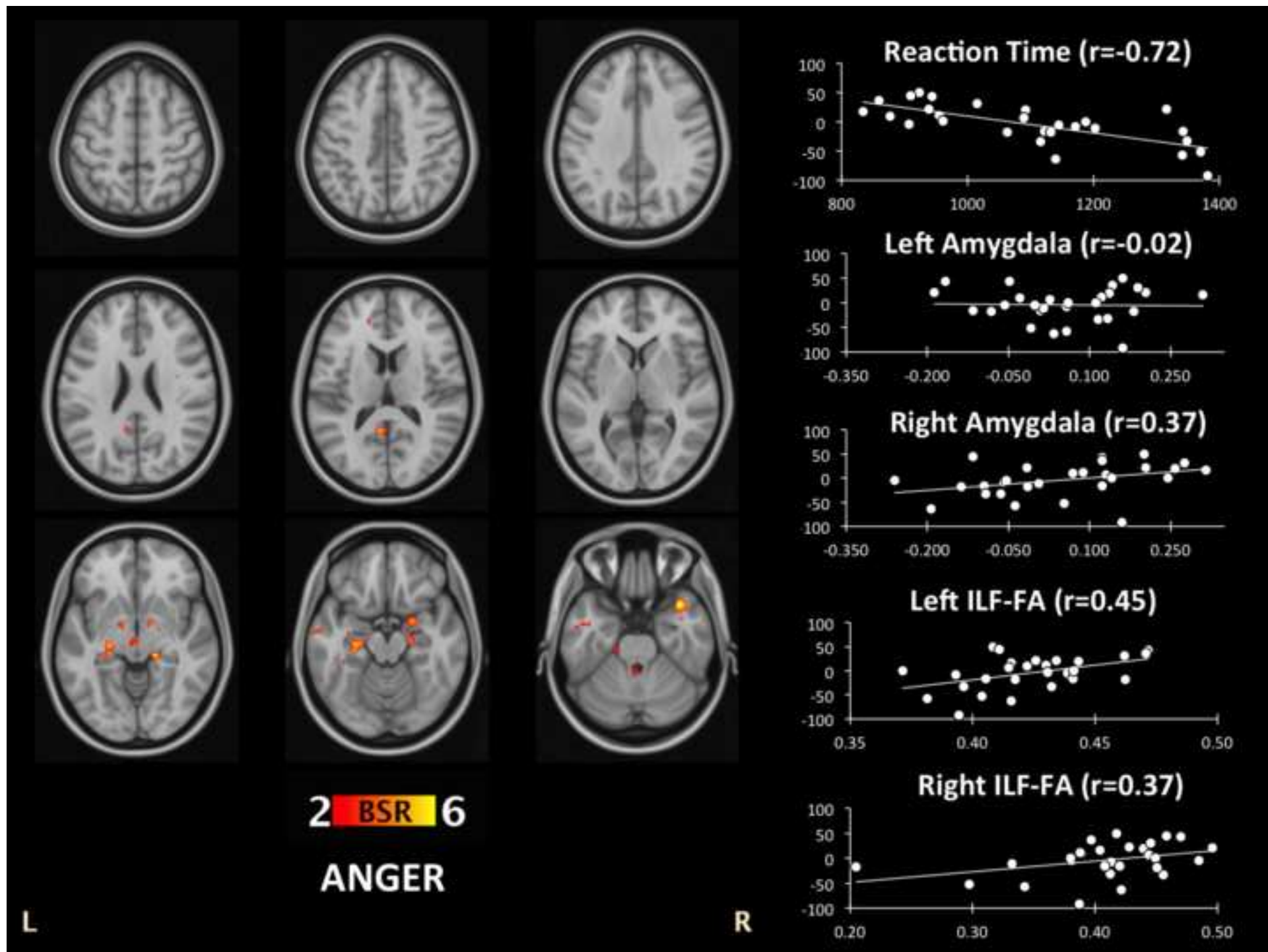


Figure 5  
[Click here to download high resolution image](#)

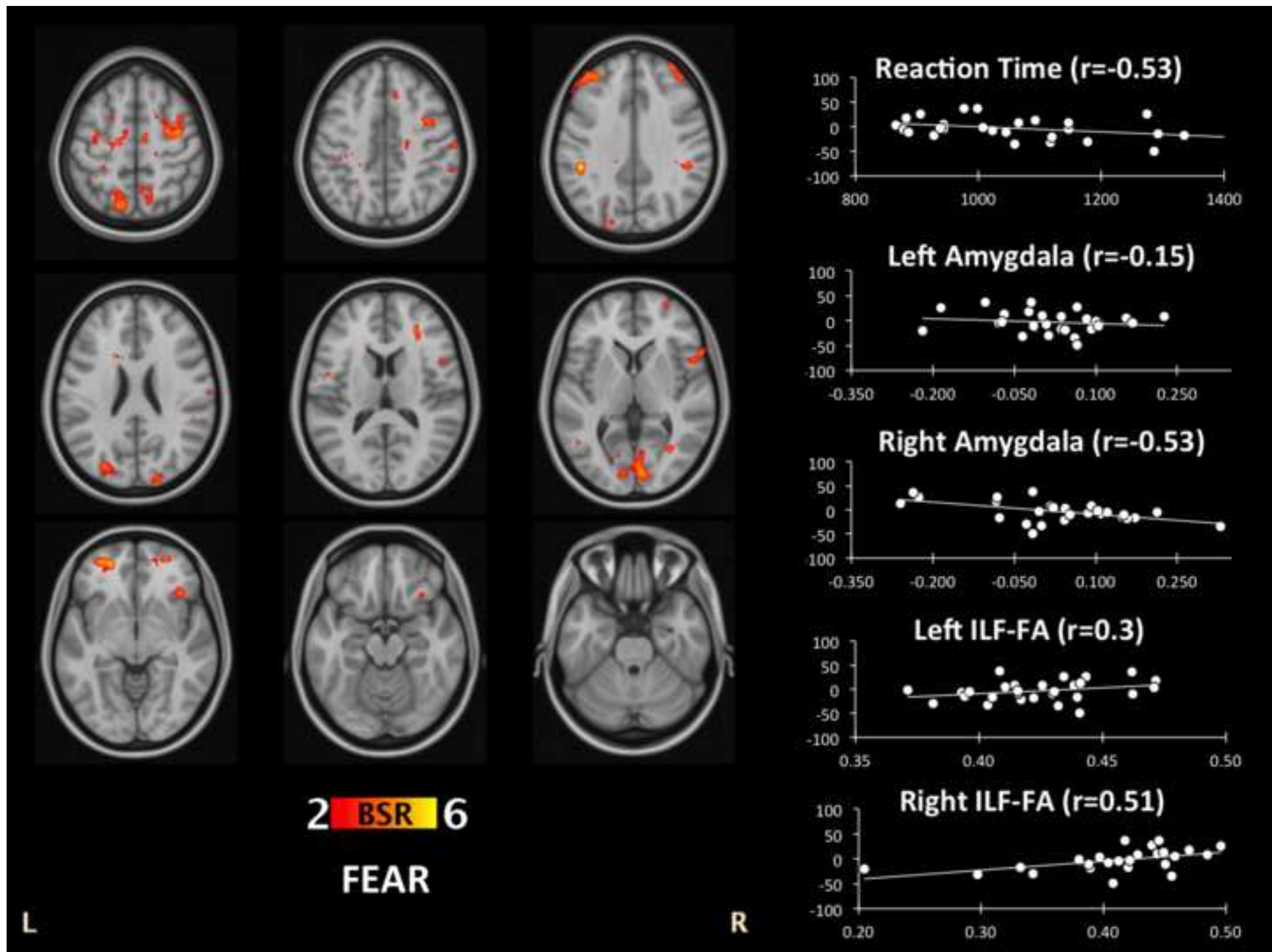




Table 1: MNI coordinates of peak voxels of whole-brain results differentiating shapes from angry and fearful face processing.

Region	Hem	MNI Coordinates			Ratio
		<i>x</i>	<i>y</i>	<i>z</i>	
<b>Shapes &gt; Angry &amp; Fearful Faces</b>					
Postcentral gyrus	L	-42	-36	54	6.1
	R	44	-36	64	7.6
Superior parietal lobule	L	-26	-46	56	6.7
<b>Angry &amp; Fearful Faces &gt; Shapes</b>					
Amygdala	L	-20	-8	-12	-4.0
	R	22	-6	-12	-4.3
Fusiform gyrus	L	-34	-50	-14	-6.8
	R	38	-46	-20	-9.4
Superior occipital cortex	L	-24	-94	0	-8.3
	R	28	-94	4	-8.1

Table 2: MNI coordinates of peak voxels of whole-brain results differentiating angry from fearful face processing.

Region	Hem	MNI Coordinates			Ratio
		<i>x</i>	<i>y</i>	<i>z</i>	
<b>Angry &gt; Fearful Faces</b>					
Middle frontal gyrus	L	-30	32	50	3.7
	R	28	34	52	5.0
Ventrolateral prefrontal cortex	R	56	26	16	4.0
Frontal orbital cortex	R	32	30	-16	3.6
Anterior cingulate cortex	L	-2	42	10	4.8
Supramarginal gyrus	R	42	-48	34	3.4
Middle temporal gyrus	L	-64	-8	-18	3.4
	R	64	-14	-16	5.3
Caudate	L	-10	12	10	4.3
<b>Fearful &gt; Angry Faces</b>					
Amygdala	R	18	-4	-18	-2.5
Pallidum	L	-12	-4	-6	-4.0
Fusiform gyrus	R	38	-46	-18	-2.3